

Local Discontinuous Galerkin Methods for Solving Convection-Diffusion and Cahn-Hilliard Equations on Surfaces

Shixin Xu · Zhiliang Xu

Received: date / Accepted: date

Abstract Local discontinuous Galerkin methods are developed for solving [second order and fourth order](#) time-dependent partial differential equations defined on [static 2D manifolds](#). These schemes are second-order accurate with surfaces triangulized by planar triangles and careful design of numerical fluxes. The schemes are proven to be energy stable. Various numerical experiments are provided to validate the new schemes.

Keywords Local discontinuous Galerkin · Manifold · Planar triangles

1 Introduction

Numerically solving partial differential equations (PDEs) defined on manifolds has drawn a lot of attention recently. This is because models of many applications, such as surface diffusion, cell membrane deformation, imaging processing and geophysical problems are formulated as second- or fourth-order partial differential equations on arbitrary surfaces or 2D Riemannian manifolds [4, 13, 14, 56, 21, 37, 38, 43, 58]. Generally speaking, numerical methods developed for solving such equations [can be classified into three categories including embedded narrow-band methods, mesh-free particle method and intrinsic methods](#) [?]. The narrow-band methods use level set method [1, 3, 5, 29, 34, 35, 41, 45, 46], kernel method [23, 46] or diffusive method [33, 42] to track the interface and the surface PDE is locally expanded. The mesh-free method employs Lagrangian framework on the surface [32, 49]. The intrinsic methods make use of an intrinsic mesh to discretize the surface and then solve the surface PDE with various numerical methods. Finite volume schemes for solving conservation laws and parabolic equations on surfaces were introduced in [26, 30, 27] and [31], respectively. Authors of papers [16, 17, 14] presented mixed finite volume methods for solving surface convection-diffusion equations and higher-order PDE. In [15], the same authors described a finite element method for solving Cahn-Hilliard equations modeling a phase separation phenomenon on surfaces. Finite element methods for solving various classes of surface PDEs were developed in [18, 19, 20, 21].

In this paper, we present local discontinuous Galerkin (LDG) methods [based on the intrinsic method](#), for solving convection-diffusion equation and Cahn-Hilliard equation on static surfaces, respectively, given that DG methods possess good stabilization mechanisms for problems which can generate steep gradients or discontinuities in their solutions. The first LDG method for solving convection-diffusion equation was introduced in [9]. Later, the LDG method for solving time-dependent PDEs with higher order derivatives was developed in [53]. In [55], A LDG method for solving Cahn-Hilliard type equations was presented. Recent papers [11, 22] described several discontinuous Galerkin (DG) formulations for solving linear elliptic

Shixin Xu

Duke Kunshan University, 8 Duke Ave, Kunshan Shi, Suzhou Shi, Jiangsu Sheng, China, 215316

Zhiliang Xu

Department of Applied and Computational Mathematics and Statistics, University of Notre Dame, Notre Dame, IN 46556
E-mail: zxu2@nd.edu

equations on surfaces, and presented a priori error estimates in the L^2 and energy norms for piecewise linear and higher-order ansatz functions and surface approximations. The hybridizable DG method to solve elliptic problems on surfaces was analyzed in [7]. Xu et al. [24,52] introduced LDG methods to solve the surface diffusion and Willmore flow on graphs (also see [2,6]). These methods are mainly based on level set representation, and the surface PDE is actually solved in 3D.

The purpose of this work is to extend the LDG method to directly solve surface PDEs posed on 2D manifolds [57]. The continuous surface Γ is approximated by a piecewise polygonal surface Γ_h . The essential ingredients of our LDG schemes consist of design of numerical fluxes motivated by [9,22,12], and the total variation diminishing (TVD) Runge-Kutta (RK) time stepping method [28,54]. To this end, we show that these schemes are energy stable. Obviously, approximating Γ by Γ_h introduces a geometric error. We do not analyze how the geometric error affects the accuracy of the solution. Instead, we presented various numerical examples. We demonstrate convergence of the fully discrete schemes for solving convection-diffusion equations and results of using the scheme for solving the Cahn-Hilliard equations defined on general surfaces. We refer readers to [21] and [27] for an analysis of geometric errors, and [11] for analyzing interior penalty (IP) DG method for elliptic problems on surfaces. We also would like to point out that authors of [12] derived a DG method for solving steady state solution of advection-dominated problems in which they used IP DG approach treating the diffusion term.

The rest of the paper is organized as follows: Section 2 describes the model equations considered in the paper. Section 3 is devoted to presenting implementation of the LDG schemes for solving the surface convection-diffusion and Cahn-Hilliard equations. Numerical tests are presented in Section 4. Finally, conclusions are drawn in Section 5.

2 Model Problems and Preliminaries

We first set basic notations. In this paper, we consider to solve initial value problems defined by two classes of equations posed on a closed and oriented two-dimensional parameterizable C^k -surface $\Gamma \subset \mathbb{R}^3$.

For later use, we assume that there exists a sufficiently thin open subset $\mathcal{N} \subset \mathbb{R}^3$ around Γ in a way that for every $\mathbf{x} \in \mathcal{N}$ there is a unique point $\zeta(\mathbf{x}) \in \Gamma$ with [19,21,27,11]

$$\mathbf{x} = \zeta(\mathbf{x}) + d(\mathbf{x})\boldsymbol{\nu}_\Gamma(\zeta(\mathbf{x})) . \quad (2.1)$$

Here d denotes the signed distance function to Γ which is assumed to be well defined in \mathcal{N} , and $\boldsymbol{\nu}_\Gamma(\zeta(\mathbf{x}))$ is the unit normal vector to Γ pointing towards the non-compact component of $\mathbb{R}^3 \setminus \Gamma$ [19,27,11]. We further assume that Γ is given locally by some diffeomorphism $X : \Omega \rightarrow \Gamma$ and some parameter domain $\Omega \subset \mathbb{R}^2$ [20].

We use the notation $X = X(\theta)$ with $\theta \in \Omega$, and introduce standard notations [21] for the first fundamental form $G(\theta) = (g_{ij}(\theta))_{i,j=1,2}$ by

$$g_{ij}(\theta) = \frac{\partial X}{\partial \theta_i}(\theta) \cdot \frac{\partial X}{\partial \theta_j}(\theta) . \quad (2.2)$$

We denote the determinant of G by $g = \det(G)$, and use superscript indices to denote the inversion of the matrix G so that

$$(g^{ij})_{i,j=1,2} = G^{-1} . \quad (2.3)$$

Definition 1 For a sufficiently smooth and differentiable function $f : \Gamma \rightarrow R$, the tangential gradient in the parametric coordinates is given by

$$\nabla_\Gamma f(X(\theta)) = \sum_{i,j=1}^2 g^{ij}(\theta) \frac{\partial f(X(\theta))}{\partial \theta_j} \frac{\partial X}{\partial \theta_i}(\theta) , \quad (2.4)$$

and the Laplace-Beltrami operator on Γ is defined by

$$\Delta_\Gamma f = \frac{1}{\sqrt{g(\theta)}} \sum_{i,j=1}^2 \frac{\partial}{\partial \theta_j} \left(g^{ij}(\theta) \sqrt{g(\theta)} \frac{\partial f(X(\theta))}{\partial \theta_i} \right) . \quad (2.5)$$

We refer readers to [21] for definitions of these operators with respect to implicitly defined surfaces and related discussion.

In this paper, the following two types of equations on surfaces will be considered:

- The time-dependent convection-diffusion equation, which is a second-order surface PDE:

$$\begin{aligned} u_t + \nabla_\Gamma \cdot (\mathbf{w}u) &= \nabla_\Gamma \cdot (a(u)\nabla_\Gamma u) , & \text{in } (0, T) \times \Gamma , \\ u(t=0) &= u_0 , & \text{on } \Gamma . \end{aligned} \quad (2.6)$$

where $a(\cdot) > 0$ and the velocity field \mathbf{w} is tangent to Γ .

- The time-dependent Cahn-Hilliard equation, which is a fourth-order surface PDE:

$$\begin{aligned} u_t &= \nabla_\Gamma \cdot (b(u)\nabla_\Gamma(-\gamma\Delta_\Gamma u + \Psi'(u))) , & \text{in } (0, T) \times \Gamma , \\ u(t=0) &= u_0 , & \text{on } \Gamma . \end{aligned} \quad (2.7)$$

where $\Psi(u)$ is the bulk homogeneous free energy density. $b(u)$ is the diffusion mobility, and γ is a positive constant.

3 Numerical Schemes

In the present work we use a triangulated surface $\Gamma_h \subset \mathcal{N}$ composed of planar triangles \mathbf{K}_h whose vertices stand on Γ to approximate Γ . Therefore,

$$\Gamma_h = \bigcup_{\mathbf{K}_h \in \mathcal{T}_h} \mathbf{K}_h ,$$

where \mathcal{T}_h denotes the set of the planar triangles which form an admissible triangulation. Notice that there exists a one-to-one relation between points $\mathbf{x} \in \Gamma_h$ and $\zeta \in \Gamma$ satisfying Eq. (2.1).

Denote by \mathcal{E} the set of edges (facets) of \mathcal{T}_h . For each $e \in \mathcal{E}$, denote by h_e the length of the edge e . Let $N_{\mathbf{K}_h}$ be an integer index of element \mathbf{K}_h , and $\mathbf{K}_h^{e,-}$ and $\mathbf{K}_h^{e,+}$ be the two elements sharing the common edge e . Denote by \mathbf{n}_h^- and \mathbf{n}_h^+ the unit outward conormal vectors defined on the edge e for $\mathbf{K}_h^{e,-}$ and $\mathbf{K}_h^{e,+}$, respectively. The conormal \mathbf{n}_h^- to a point $\mathbf{x} \in e$ is defined as follows [22]

- the unique unit vector that lies in the plane containing $\mathbf{K}_h^{e,-}$;
- $\mathbf{n}_h^-(\mathbf{x}) \cdot (\mathbf{x} - \mathbf{y}) \geq 0$, $\forall \mathbf{y} \in \mathbf{K}_h^{e,-} \cap B_\epsilon(\mathbf{x})$, where $B_\epsilon(\mathbf{x})$ is a ball centered in \mathbf{x} . The radius $\epsilon (> 0)$ of $B_\epsilon(\mathbf{x})$ is sufficiently small.

The conormal \mathbf{n}_h^+ is defined similarly. With this definition, we have

$$\mathbf{n}_h^+ \neq -\mathbf{n}_h^-$$

in general (See Fig. 1 for example).

Let $\mathbb{P}_k(D)$ denote the space of polynomials of degree not greater than k on any planar domain D . The discrete DG space $\mathbb{S}_{h,k}$ of scalar function associated with Γ_h is

$$\mathbb{S}_{h,k} = \{ \chi \in L^2(\Gamma_h) : \chi|_{\mathbf{K}_h} \in \mathbb{P}_k(\mathbf{K}_h), \forall \mathbf{K}_h \in \mathcal{T}_h \} ,$$

i.e. the space of piecewise polynomials which are globally in $L^2(\Gamma_h)$.

The vector-valued DG space $\boldsymbol{\Sigma}_{h,k}$ associated with Γ_h is chosen to be

$$\boldsymbol{\Sigma}_{h,k} = \left\{ \boldsymbol{\varphi} \in [L^2(\Gamma_h)]^3 : \boldsymbol{\varphi}|_{\mathbf{K}_h} \in [\mathbb{P}_k(\mathbf{K}_h)]^3, \forall \mathbf{K}_h \in \mathcal{T}_h \right\} .$$

For $v_h \in \mathbb{S}_{h,k}$ and $\mathbf{r}_h \in \boldsymbol{\Sigma}_{h,k}$, we use v_h^\pm and \mathbf{r}_h^\pm to denote the trace of v_h and \mathbf{r}_h on $e = \mathbf{K}_h^{e,+} \cap \mathbf{K}_h^{e,-}$ taken within the interior of $\mathbf{K}_h^{e,+}$ and $\mathbf{K}_h^{e,-}$, respectively.

For a given function $f_h \in \mathbb{S}_{h,k}$, the surface gradient operator on Γ_h denoted by ∇_{Γ_h} and the laplace-Beltrami operator on Γ_h denoted by Δ_{Γ_h} are defined similarly as in Def. 1.

For the purpose of analysis, we further introduce a lift onto Γ for any function v_h defined on the discrete surface Γ_h as follows.

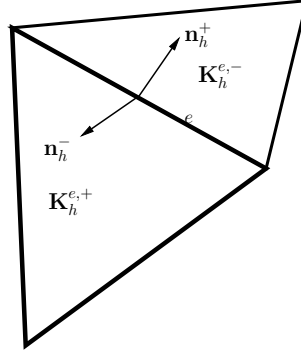


Fig. 1 Two elements $\mathbf{K}_h^{e,+}$ and $\mathbf{K}_h^{e,-}$ and their respective conormals \mathbf{n}_h^+ and \mathbf{n}_h^- on the common edge e .

Definition 2 For any function $v_h \in \mathbb{S}_{h,k}$ defined on Γ_h , the lift or extension [21] onto Γ is given by:

$$v_h^l(\zeta) := v_h(\mathbf{x}(\zeta)), \quad \zeta \in \Gamma,$$

where $\mathbf{x}(\zeta)$ is the unique solution of Eq. (2.1).

Also by Def. 2, for every $\mathbf{K}_h \subset \Gamma_h$, there is a unique curved triangle $\mathbf{K}_h^l = \zeta(\mathbf{K}_h) \subset \Gamma$. When transforming from Γ_h to Γ , denote by δ_h the quotient between the smooth and discrete surface measures dA on Γ and dA_h on Γ_h so that $\delta_h dA_h = dA$, and δ_e the quotient between measures ds_h on e and ds on e^l so that $\delta_e ds_h = ds$.

$\mathbb{S}_{h,k}^l$, the lifted finite element space is defined as

$$\mathbb{S}_{h,k}^l = \{ \phi_h = \varphi_h^l | \varphi_h \in \mathbb{S}_{h,k} \}. \quad (3.8)$$

The lifted space $\mathbb{\Sigma}_{h,k}^l$ is defined similarly.

3.1 LDG Method for Surface Convection-Diffusion Equation

By introducing the auxiliary variable $\mathbf{q} = \sqrt{a(u)} \nabla_{\Gamma} u$, the model problem (2.6) can be rewritten as a first order system of equations:

$$\begin{cases} u_t + \nabla_{\Gamma} \cdot (u \mathbf{w} - \sqrt{a(u)} \mathbf{q}) = 0, \\ \mathbf{q} - \nabla_{\Gamma} g(u) = 0, \end{cases} \quad (3.9)$$

where $g(u) = \int^u \sqrt{a(s)} ds$.

The LDG method for solving Eqs. (3.9) is defined by: Find $u_h \in \mathbb{S}_{h,k}$ and $\mathbf{q}_h \in \mathbb{\Sigma}_{h,k}$, such that for all test functions $v_h \in \mathbb{S}_{h,k}$ and $\mathbf{r}_h \in \mathbb{\Sigma}_{h,k}$,

$$\begin{cases} \int_{\mathbf{K}_h} (u_h)_t v_h d\mathbf{x} - \int_{\mathbf{K}_h} (u_h \mathbf{w}_h - \sqrt{a(u)} \mathbf{q}_h) \cdot \nabla_{\Gamma_h} v_h d\mathbf{x} + \int_{\mathbf{K}_h} (\beta_h u_h v_h) d\mathbf{x} \\ \quad + \int_{\partial \mathbf{K}_h} \widehat{u_h \mathbf{w}_h} \cdot \mathbf{n}_h v_h ds - \int_{\partial \mathbf{K}_h} \widehat{\sqrt{a} \mathbf{q}} \cdot \mathbf{n}_h v_h ds = 0, \\ \int_{\mathbf{K}_h} \mathbf{q}_h \cdot \mathbf{r}_h d\mathbf{x} = - \int_{\mathbf{K}_h} g(u_h) \nabla_{\Gamma_h} \cdot \mathbf{r}_h d\mathbf{x} + \int_{\partial \mathbf{K}_h} \widehat{g} \mathbf{n}_h \cdot \mathbf{r}_h ds. \end{cases} \quad (3.10)$$

Here \widehat{g} , $\widehat{\sqrt{a} \mathbf{q}}$ and $\widehat{u_h \mathbf{w}_h}$ are numerical fluxes which will be prescribed later on. \mathbf{w}_h , defined on Γ_h , is a surface Raviart-Thomas interpolant of \mathbf{w} such that normal jumps of the velocity across edges will vanish, namely, $\mathbf{w}_h^- \cdot \mathbf{n}_h^- + \mathbf{w}_h^+ \cdot \mathbf{n}_h^+ = 0$. The method to compute \mathbf{w}_h is described in [12]. The term containing β_h is for stability, and β_h is defined to be:

$$\beta_h = \begin{cases} 0, & \text{if } \nabla_{\Gamma_h} \cdot \mathbf{w}_h \geq 0; \\ -\frac{1}{2} \nabla_{\Gamma_h} \cdot \mathbf{w}_h, & \text{if } \nabla_{\Gamma_h} \cdot \mathbf{w}_h < 0. \end{cases} \quad (3.11)$$

To facilitate definitions of numerical fluxes, following trace operators $\{\cdot\}$ and $[\![\cdot]\!]$ are introduced by following ideas in [22].

Definition 3 Denote by $\mathbf{K}_h^{e,+}$ and $\mathbf{K}_h^{e,-}$ the two elements sharing the common edge e .

– For $v \in L^2(\Gamma_h)$, $\{v\}$ and $[\![v]\!]$ are defined as

$$\{v\} = \frac{1}{2}(v^- + v^+) , \quad [\![v]\!] = v^+ - v^- \text{ on } e. \quad (3.12)$$

– For $\varphi \in [L^2(\Gamma_h)]^3$, $\{\varphi, \mathbf{n}_h\}$ and $[\![\varphi, \mathbf{n}_h]\!]$ are defined as

$$\{\varphi, \mathbf{n}_h\} = \frac{1}{2}(\varphi^+ \cdot \mathbf{n}_h^+ - \varphi^- \cdot \mathbf{n}_h^-) , \quad [\![\varphi, \mathbf{n}_h]\!] = \varphi^- \cdot \mathbf{n}_h^- + \varphi^+ \cdot \mathbf{n}_h^+ \text{ on } e. \quad (3.13)$$

Denote by $S_{\mathbf{K}_h^+}^{\mathbf{K}_h^-} \in \{0, 1\}$ a switch function [40]. $S_{\mathbf{K}_h^+}^{\mathbf{K}_h^-}$ is associated with \mathbf{K}_h^+ on the edge that \mathbf{K}_h^+ and \mathbf{K}_h^- share, and is defined by:

$$S_{\mathbf{K}_h^+}^{\mathbf{K}_h^-} = \begin{cases} 1 , & \text{if } N_{\mathbf{K}_h^+} > N_{\mathbf{K}_h^-} , \\ 0 , & \text{otherwise .} \end{cases} \quad (3.14)$$

Motivated by [9,22,12], the numerical fluxes on e for $\mathbf{K}_h^{e,+}$ and $\mathbf{K}_h^{e,-}$ are defined respectively, as follows.

– The convective fluxes $\widehat{u_h \mathbf{w}_h}^+$ and $\widehat{u_h \mathbf{w}_h}^-$:

$$\begin{aligned} \widehat{u_h \mathbf{w}_h}^+ &= (\{u_h \mathbf{w}_h, \mathbf{n}_h\} + \frac{\alpha}{2} [u_h]) \mathbf{n}_h^+ , \\ \widehat{u_h \mathbf{w}_h}^- &= -(\{u_h \mathbf{w}_h, \mathbf{n}_h\} + \frac{\alpha}{2} [u_h]) \mathbf{n}_h^- , \end{aligned} \quad (3.15)$$

where $\alpha = \max |\mathbf{n}_h \cdot \mathbf{w}_h|$.

– The diffusive fluxes $(\widehat{\sqrt{a} \mathbf{q}}^+, \widehat{g}^+)^T$ and $(\widehat{\sqrt{a} \mathbf{q}}^-, \widehat{g}^-)^T$:

$$\begin{aligned} \widehat{\sqrt{a} \mathbf{q}}^+ &= \left(\frac{[g(u_h)]}{[u_h]} \{\mathbf{q}_h, \mathbf{n}_h\} - C_{11} [u_h] + C_{12} \cdot \mathbf{n}_h^+ [\mathbf{q}_h, \mathbf{n}_h] \right) \mathbf{n}_h^+ \\ \widehat{\sqrt{a} \mathbf{q}}^- &= - \left(\frac{[g(u_h)]}{[u_h]} \{\mathbf{q}_h, \mathbf{n}_h\} - C_{11} [u_h] + C_{12} \cdot \mathbf{n}_h^+ [\mathbf{q}_h, \mathbf{n}_h] \right) \mathbf{n}_h^- . \end{aligned} \quad (3.16)$$

$$\begin{aligned} \widehat{g}^+ &= \{g(u_h)\} - C_{12} \cdot \mathbf{n}_h^+ [u_h] , \\ \widehat{g}^- &= \{g(u_h)\} - C_{12} \cdot \mathbf{n}_h^+ [u_h] . \end{aligned} \quad (3.17)$$

Here the penalization coefficients C_{11} and C_{12} are chosen to be

$$C_{11} = \frac{1}{h_e} , \quad C_{12} = \frac{1}{2} \left(S_{\mathbf{K}_h^{e,+}}^{\mathbf{K}_h^{e,-}} \mathbf{n}_h^+ + S_{\mathbf{K}_h^{e,-}}^{\mathbf{K}_h^{e,+}} \mathbf{n}_h^- \right) .$$

It is easy to see that with the above choices of the numerical fluxes, $[\![\widehat{u_h \mathbf{w}_h}, \mathbf{n}]\!] = 0$, $[\![\widehat{g}]\!] = 0$ and $[\![\widehat{\sqrt{a} \mathbf{q}}, \mathbf{n}]\!] = 0$. Thus these numerical fluxes are consistent and conservative. Moreover, they allow for a local resolution of \mathbf{q}_h in terms of u_h .

We introduce the surface H^1 space $H^1(\Gamma_h) = \{v |_{\mathbf{K}_h} \in H^1(\mathbf{K}_h), \forall \mathbf{K}_h \in \Gamma_h\}$. The following Lemma is needed for analyzing the L^2 -stability of the scheme (3.10).

Lemma 1 ([22]) Let $v \in H^1(\Gamma_h)$ and $\mathbf{r} \in [H^1(\Gamma_h)]^3$. Then

$$\sum_{\mathbf{K}_h \in \Gamma_h} \int_{\partial \mathbf{K}_h} \mathbf{v} \mathbf{r} \cdot \mathbf{n}_h ds = \sum_{e \in \mathcal{E}} \int_e [\![\mathbf{r}, \mathbf{n}_h]\!] \{v\} + \{\mathbf{r}, \mathbf{n}_h\} [\![v]\!] ds . \quad (3.18)$$

The following estimate holds for the LDG scheme (3.10) to solve the surface convection-diffusion equation (2.6).

Proposition 1 (*L^2 -stability of LDG scheme (3.10)*) Let $(u_h, \mathbf{q}_h)^T$ be a solution of the scheme (3.10) with initial value $u_h(\mathbf{x}, t=0)$ given by L^2 projection of u_0 , and $(u_t^l, \mathbf{q}_h^l)^T$ its lift according to Definition 2. Then the following stability estimate holds:

$$\begin{aligned} & \frac{1}{2} \int_{\Gamma} \frac{1}{\delta_h} (u_h^l)^2(\mathbf{x}, T) d\mathbf{x} + \int_0^T \int_{\Gamma} \frac{1}{\delta_h} |\mathbf{q}_h^l(\mathbf{x}, t)|^2 dxdt + \Theta_{T,C}([\mathcal{W}_h^l]) \\ & \leq \frac{1}{2} \int_{\Gamma} \frac{1}{\delta_h} (u_0)^2(\mathbf{x}) d\mathbf{x}, \end{aligned} \quad (3.19)$$

where $\mathcal{W}_h^l = (u_h^l, \mathbf{q}_h^l)^T$ and $\Theta_{T,C}([\mathcal{W}_h^l]) = \int_0^T \sum_{e^l \in \mathcal{E}^l} \int_{e^l} \frac{1}{\delta_e} \left(C_{11} + \frac{\alpha}{2} \right) [u_h^l]^2 dsdt$.

Proof of Proposition 1 follows directly from [9, 19, 12], and is briefly described below.

Proof Denote by $\mathcal{W}_h = (u_h, \mathbf{q}_h)^T$ and $\mathcal{V}_h = (v_h, \mathbf{r}_h)^T$. Let's first define a functional by adding two component equations of Eq. (3.10) up, and summing over all elements:

$$\begin{aligned} 0 &= \mathcal{A}_h(\mathcal{W}_h, \mathcal{V}_h) \\ &= \sum_{\mathbf{K}_h \in \Gamma_h} \int_{\mathbf{K}_h} (u_h)_t v_h d\mathbf{x} - \sum_{\mathbf{K}_h \in \Gamma_h} \int_{\mathbf{K}_h} u_h \mathbf{w}_h \cdot \nabla_{\Gamma_h} v_h d\mathbf{x} + \sum_{\mathbf{K}_h \in \Gamma_h} \int_{\mathbf{K}_h} \mathbf{q}_h \cdot \mathbf{r}_h d\mathbf{x} \\ &+ \sum_{\mathbf{K}_h \in \Gamma_h} \int_{\mathbf{K}_h} \sqrt{a} \mathbf{q}_h \cdot \nabla_{\Gamma_h} v_h d\mathbf{x} + \sum_{\mathbf{K}_h \in \Gamma_h} \int_{\mathbf{K}_h} g(u_h) \nabla_{\Gamma_h} \cdot \mathbf{r}_h d\mathbf{x} \\ &+ \sum_{\mathbf{K}_h \in \Gamma_h} \int_{\mathbf{K}_h} \beta_h u_h v_h d\mathbf{x} + \sum_{\mathbf{K}_h \in \Gamma_h} \int_{\partial \mathbf{K}_h} v_h \widehat{u_h \mathbf{w}_h} \cdot \mathbf{n}_h ds \\ &+ \sum_{\mathbf{K}_h \in \Gamma_h} \int_{\partial \mathbf{K}_h} (-\widehat{\sqrt{a} \mathbf{q}}) \cdot \mathbf{n}_h v_h ds - \sum_{\mathbf{K}_h \in \Gamma_h} \int_{\partial \mathbf{K}_h} \widehat{g \mathbf{n}_h} \cdot \mathbf{r}_h ds. \end{aligned} \quad (3.20)$$

By replacing $v_h(\mathbf{x})$ and $\mathbf{r}_h(\mathbf{x})$ by $u_h(\mathbf{x}, t)$ and $\mathbf{q}_h(\mathbf{x}, t)$ in Eq. (3.20), integrating from 0 to T , and using Lemma 1 and Eqs. (3.15) - (3.17), it can be shown that

$$\begin{aligned} 0 &= \int_0^T \mathcal{A}_h(\mathbf{w}_h, \mathbf{w}_h) dt \\ &= \int_0^T \sum_{\mathbf{K}_h \in \Gamma_h} \int_{\mathbf{K}_h} (u_h)_t u_h dxdt + \int_0^T \sum_{\mathbf{K}_h \in \Gamma_h} \int_{\mathbf{K}_h} |\mathbf{q}_h|^2 dxdt \\ &- \int_0^T \sum_{\mathbf{K}_h \in \Gamma_h} \int_{\mathbf{K}_h} u_h \mathbf{w}_h \cdot \nabla_{\Gamma_h} u_h dxdt + \int_0^T \sum_{\mathbf{K}_h \in \Gamma_h} \int_{\partial \mathbf{K}_h} u_h \widehat{u_h \mathbf{w}_h} \cdot \mathbf{n}_h dsdt \\ &+ \int_0^T \sum_{e \in \mathcal{E}} \int_e C_{11} [u_h]^2 dsdt + \int_0^T \sum_{\mathbf{K}_h \in \Gamma_h} \int_{\mathbf{K}_h} \beta_h u_h^2 dxdt \\ &= \frac{1}{2} \int_{\Gamma_h} (u_h)^2(\mathbf{x}, T) dxdt - \frac{1}{2} \int_{\Gamma_h} (u_h)^2(\mathbf{x}, 0) dxdt \\ &+ \int_0^T \int_{\Gamma_h} |\mathbf{q}_h|^2 dxdt + \int_0^T \sum_{e \in \mathcal{E}} \int_e C_{11} [u_h]^2 dsdt \\ &+ \int_0^T \sum_{\mathbf{K}_h \in \Gamma_h} \int_{\mathbf{K}_h} \beta_h u_h^2 dxdt - \int_0^T \sum_{\mathbf{K}_h \in \Gamma_h} \int_{\mathbf{K}_h} u_h \mathbf{w}_h \cdot \nabla_{\Gamma_h} u_h dxdt \\ &+ \int_0^T \sum_{\mathbf{K}_h \in \Gamma_h} \int_{\partial \mathbf{K}_h} u_h \widehat{u_h \mathbf{w}_h} \cdot \mathbf{n}_h dsdt \end{aligned} \quad (3.21)$$

Define by

$$\begin{aligned} & \mathcal{B}_h(\mathcal{W}_h, \mathcal{W}_h) \\ &= - \int_0^T \sum_{\mathbf{K}_h \in \Gamma_h} \int_{\mathbf{K}_h} u_h \mathbf{w}_h \cdot \nabla_{\Gamma_h} u_h dxdt + \int_0^T \sum_{\mathbf{K}_h \in \Gamma_h} \int_{\partial \mathbf{K}_h} u_h \widehat{u_h \mathbf{w}_h} \cdot \mathbf{n}_h dsdt. \end{aligned}$$

By integrating by parts on each \mathbf{K}_h for the first term of $\mathcal{B}_h(\mathcal{W}_h, \mathcal{W}_h)$ and using $[[\mathbf{w}_h, \mathbf{n}_h]] = 0$ and Eq. (3.15), we obtain

$$\begin{aligned}
& \mathcal{B}_h(\mathcal{W}_h, \mathcal{W}_h) \\
&= -\frac{1}{2} \int_0^T \sum_{\mathbf{K}_h \in \Gamma_h} \int_{\partial \mathbf{K}_h} (u_h)^2 \mathbf{w}_h \cdot \mathbf{n}_h ds dt + \frac{1}{2} \int_0^T \sum_{\mathbf{K}_h \in \Gamma_h} \int_{\mathbf{K}_h} u_h^2 \nabla_{\Gamma_h} \cdot \mathbf{w}_h dx dt \\
&\quad + \int_0^T \sum_{\mathbf{K}_h \in \Gamma_h} \int_{\partial \mathbf{K}_h} u_h \widehat{u_h \mathbf{w}_h} \cdot \mathbf{n}_h ds dt \\
&= -\frac{1}{2} \int_0^T \sum_{e \in \mathcal{E}} \int_e ([[\mathbf{w}_h, \mathbf{n}_h]] \{u_h^2\} + \{ \mathbf{w}_h, \mathbf{n}_h \} [[u_h^2]]) ds dt \\
&\quad + \int_0^T \sum_{e \in \mathcal{E}} \int_e (\{u_h \mathbf{w}_h, \mathbf{n}_h\} + \frac{\alpha}{2} [[u_h]]) [[u_h]] ds dt + \frac{1}{2} \int_0^T \sum_{\mathbf{K}_h \in \Gamma_h} \int_{\mathbf{K}_h} u_h^2 \nabla_{\Gamma_h} \cdot \mathbf{w}_h dx dt \\
&= -\frac{1}{2} \int_0^T \sum_{e \in \mathcal{E}} \int_e (\{ \mathbf{w}_h, \mathbf{n}_h \} [[u_h^2]]) ds dt \\
&\quad + \int_0^T \sum_{e \in \mathcal{E}} \int_e (\frac{1}{2} \{ \mathbf{w}_h, \mathbf{n}_h \} [[u_h^2]] + \frac{\alpha}{2} [[u_h]]^2) ds dt + \frac{1}{2} \int_0^T \sum_{\mathbf{K}_h \in \Gamma_h} \int_{\mathbf{K}_h} u_h^2 \nabla_{\Gamma_h} \cdot \mathbf{w}_h dx dt .
\end{aligned} \tag{3.22}$$

This leads to

$$\begin{aligned}
\int_0^T \mathcal{A}_h(\mathbf{w}_h, \mathbf{w}_h) dt &= \frac{1}{2} \int_{\Gamma_h} (u_h)^2(\mathbf{x}, T) dx - \frac{1}{2} \int_{\Gamma_h} (u_h)^2(\mathbf{x}, 0) dx \\
&\quad + \int_0^T \int_{\Gamma_h} |\mathbf{q}_h|^2 dx dt + \int_0^T \sum_{e \in \mathcal{E}} \int_e (\frac{\alpha}{2} + C_{11}) [[u_h]]^2 ds dt .
\end{aligned} \tag{3.23}$$

Since $\int_{\Gamma_h} (u_h)^2(\mathbf{x}, 0) dx \leq \int_{\Gamma_h} (u_0)^2 dx$ (by Lemma 4.2 in [21]), it gives rise to:

$$\begin{aligned}
& \frac{1}{2} \int_{\Gamma_h} (u_h)^2(\mathbf{x}, T) dx + \int_0^T \int_{\Gamma_h} |\mathbf{q}_h|^2 dx dt + \int_0^T \sum_{e \in \mathcal{E}} \int_e (\frac{\alpha}{2} + C_{11}) [[u_h]]^2 ds dt \\
& \leq \frac{1}{2} \int_{\Gamma_h} (u_h)^2(\mathbf{x}, 0) dx .
\end{aligned} \tag{3.24}$$

By lifting u_h and \mathbf{q}_h onto surface Γ , it is shown that

$$\begin{aligned}
& \frac{1}{2} \int_{\Gamma} \frac{1}{\delta_h} (u_h^l)^2(\mathbf{x}, T) dx + \int_0^T \int_{\Gamma} \frac{1}{\delta_h} |\mathbf{q}_h^l|^2 dx dt + \int_0^T \sum_{e \in \mathcal{E}} \int_e \frac{1}{\delta_e} (\frac{\alpha}{2} + C_{11}) [[u_h]]^2 ds dt \\
& \leq \frac{1}{2} \int_{\Gamma} \frac{1}{\delta_h} (u_0)^2(\mathbf{x}, 0) dx .
\end{aligned} \tag{3.25}$$

3.2 LDG Method for Cahn-Hilliard Equation

In order to solve the model problem (2.7) by the LDG method, the equation is rewritten as a first order system of [equations](#):

$$\begin{cases} u_t = \nabla_{\Gamma} \cdot \mathbf{S} , \\ \mathbf{S} = b(u) \mathbf{P} , \\ \mathbf{P} = \nabla_{\Gamma} (-q + r) , \\ q = \gamma \nabla_{\Gamma} \cdot \mathbf{W} , \\ \mathbf{W} = \nabla_{\Gamma} u , \\ r = \Psi'(u) . \end{cases} \tag{3.26}$$

The LDG scheme for solving Eqs. (3.26) is as follows: Find $u_h, q_h, r_h \in \mathbb{S}_{h,k}$ and $\mathbf{S}_h, \mathbf{P}_h, \mathbf{W}_h \in \boldsymbol{\Sigma}_{h,k}$, such that for all test functions $v_h, \varphi_h, \xi_h \in \mathbb{S}_{h,k}$ and $\boldsymbol{\Theta}_h, \boldsymbol{\Phi}_h, \boldsymbol{\Upsilon}_h \in \boldsymbol{\Sigma}_{h,k}$,

$$\left\{ \begin{array}{l} \int_{\mathbf{K}_h} (u_h)_t v_h d\mathbf{x} + \int_{\mathbf{K}_h} \mathbf{S}_h \cdot \nabla_{\Gamma_h} v_h d\mathbf{x} - \int_{\partial\mathbf{K}_h} \widehat{\mathbf{S}} \cdot \mathbf{n}_h v_h ds = 0, \\ \int_{\mathbf{K}_h} \mathbf{S}_h \cdot \boldsymbol{\Theta}_h d\mathbf{x} = \int_{\mathbf{K}_h} b(u_h) \mathbf{P}_h \cdot \boldsymbol{\Theta}_h d\mathbf{x}, \\ \int_{\mathbf{K}_h} \mathbf{P}_h \cdot \boldsymbol{\Phi}_h d\mathbf{x} = - \int_{\mathbf{K}_h} (-q_h + r_h) \nabla_{\Gamma_h} \cdot \boldsymbol{\Phi}_h d\mathbf{x} + \int_{\partial\mathbf{K}_h} (\widehat{r} - \widehat{q}) \mathbf{n}_h \cdot \boldsymbol{\Phi}_h ds, \\ \int_{\mathbf{K}_h} q_h \varphi_h d\mathbf{x} = -\gamma \int_{\mathbf{K}_h} \mathbf{W}_h \cdot \nabla_{\Gamma_h} \varphi_h d\mathbf{x} + \gamma \int_{\partial\mathbf{K}_h} \widehat{\mathbf{W}} \cdot \mathbf{n}_h \varphi_h ds, \\ \int_{\mathbf{K}_h} \mathbf{W}_h \cdot \boldsymbol{\Upsilon}_h d\mathbf{x} = - \int_{\mathbf{K}_h} u_h \nabla_{\Gamma_h} \cdot \boldsymbol{\Upsilon}_h d\mathbf{x} + \int_{\partial\mathbf{K}_h} \widehat{u} \mathbf{n}_h \cdot \boldsymbol{\Upsilon}_h ds \\ \int_{\mathbf{K}_h} r_h \xi_h d\mathbf{x} = \int_{\mathbf{K}_h} \Psi'(u_h) \xi_h d\mathbf{x}. \end{array} \right. \quad (3.27)$$

Following ideas in [9,22,55] the numerical fluxes on e for $\mathbf{K}_h^{e,+}$ and $\mathbf{K}_h^{e,-}$ for solving the system (3.27) are defined by:

$$\begin{aligned} \widehat{\mathbf{S}}^+ &= (\{\mathbf{S}_h, \mathbf{n}\} - C_{11} \llbracket u_h \rrbracket + C_{12} \cdot \mathbf{n}_h^+ \llbracket \mathbf{S}_h, \mathbf{n} \rrbracket) \mathbf{n}_h^+, \\ \widehat{\mathbf{S}}^- &= -(\{\mathbf{S}_h, \mathbf{n}\} - C_{11} \llbracket u_h \rrbracket + C_{12} \cdot \mathbf{n}_h^+ \llbracket \mathbf{S}_h, \mathbf{n} \rrbracket) \mathbf{n}_h^-. \end{aligned} \quad (3.28)$$

$$\begin{aligned} \widehat{u}^+ &= \{u_h\} - C_{12} \cdot \mathbf{n}_h^+ \llbracket u_h \rrbracket \\ \widehat{u}^- &= \{u_h\} - C_{12} \cdot \mathbf{n}_h^+ \llbracket u_h \rrbracket. \end{aligned} \quad (3.29)$$

$$\begin{aligned} \widehat{\mathbf{W}}^+ &= (\{\mathbf{W}_h, \mathbf{n}\} - C_{11} \llbracket u_h \rrbracket + C_{12} \cdot \mathbf{n}_h^+ \llbracket \mathbf{W}_h, \mathbf{n} \rrbracket) \mathbf{n}_h^+, \\ \widehat{\mathbf{W}}^- &= -(\{\mathbf{W}_h, \mathbf{n}\} - C_{11} \llbracket u_h \rrbracket + C_{12} \cdot \mathbf{n}_h^+ \llbracket \mathbf{W}_h, \mathbf{n} \rrbracket) \mathbf{n}_h^-. \end{aligned} \quad (3.30)$$

$$\begin{aligned} \widehat{r}^+ &= \{r_h\} - C_{12} \cdot \mathbf{n}_h^+ \llbracket r_h \rrbracket, \\ \widehat{r}^- &= \{r_h\} - C_{12} \cdot \mathbf{n}_h^+ \llbracket r_h \rrbracket. \end{aligned} \quad (3.31)$$

$$\begin{aligned} \widehat{q}^+ &= \{q_h\} - C_{12} \cdot \mathbf{n}_h^+ \llbracket q_h \rrbracket, \\ \widehat{q}^- &= \{q_h\} - C_{12} \cdot \mathbf{n}_h^+ \llbracket q_h \rrbracket. \end{aligned} \quad (3.32)$$

Proposition 2 (energy stability of LDG scheme (3.27)) *The solution to the scheme (3.27) satisfies the energy stability*

$$\frac{d}{dt} \int_{\Gamma} \frac{1}{\delta_h} \left(\frac{\gamma}{2} \mathbf{W}_h^l \cdot \mathbf{W}_h^l + \Psi(u_h^l) \right) d\mathbf{x} \leq 0.$$

Proof Following the proof in [55], it can be shown that

$$\frac{d}{dt} \int_{\Gamma_h} \left(\frac{\gamma}{2} \mathbf{W}_h \cdot \mathbf{W}_h + \Psi(u_h) \right) d\mathbf{x} \leq 0. \quad (3.33)$$

By lifting u_h and \mathbf{W}_h onto surface Γ , it yields:

$$\frac{d}{dt} \int_{\Gamma} \frac{1}{\delta_h} \left(\frac{\gamma}{2} \mathbf{W}_h^l \cdot \mathbf{W}_h^l + \Psi(u_h^l) \right) d\mathbf{x} \leq 0. \quad (3.34)$$

3.3 Time discretization

The method of lines spatial approximation to PDEs is used for discretization and the time t is left to be continuous till now. The second-order accurate TVD RK time discretization [54,28] is used to solve the semi-discrete schemes (3.10) and (3.27), which can be formulated as an ordinary differential equation:

$$\Phi_t = L(\Phi, t) . \quad (3.35)$$

The second-order accurate TVD RK method for solving Eq. (3.35) is given by

$$\begin{aligned} \Phi^{(1)} &= \Phi^n + \Delta t_n L(\Phi^n, t_n) , \\ \Phi^{n+1} &= \frac{1}{2}\Phi^n + \frac{1}{2}\Phi^{(1)} + \frac{1}{2}\Delta t_n L(\Phi^{(1)}, t_{n+1}) . \end{aligned} \quad (3.36)$$

Here Δt_n is the time step size.

Remark 1 *In this paper, we only considered planar triangulations of the surface Γ , which is at most second-order accurate. Therefore, we choose the second-order accurate TVD RK time-stepping method. Higher-order accurate surface approximation is needed in order to improve the overall accuracy of the schemes.*

4 Numerical results

Numerical experiments based on the schemes defined in Sec. 3 are presented in this section. All meshes used here are generated by MATLAB program DistMesh [39]. The CFL condition for LDG scheme for convection-diffusion equation is

$$\min \left(\frac{\max |\mathbf{w}_h| \Delta t_n}{h_e}, \frac{\max(a'(u)) \Delta t_n}{h_e^2} \right) \leq C_{CFL} , \quad (4.37)$$

C_{CFL} is the CFL number. The time step size for LDG scheme for Cahn-Hilliard equation is:

$$\Delta t_n = \mathcal{O}(h_e^4) . \quad (4.38)$$

4.1 Linear advection on a sphere

We first illustrate the convergence rate of the numerical scheme by using the test problem 6 described in [27]. This test problem solves

$$\frac{\partial u}{\partial t} + \nabla_{\Gamma} \cdot (u \mathbf{V}) = 0 , \quad t \in (0, 1] , \quad (4.39)$$

defined on a unit spherical surface given by

$$\mathbb{S}_1 = \{ \mathbf{x} \in \mathbb{R}^3 \mid x_1^2 + x_2^2 + x_3^2 = 1 \} .$$

The divergence-free advecting velocity field $\mathbf{V} = (v_1, v_2, v_3)^T$ at position $\mathbf{x} = (x_1, x_2, x_3)^T$ is given by $\mathbf{V} = \frac{2\pi}{\|\mathbf{x}\|} (x_2, -x_1, 0)^T$. The initial condition is given by

$$u_0(\mathbf{x}) = \begin{cases} \frac{1}{10} \exp \left(\frac{-2(1+r^2(\mathbf{x}))}{(1-r^2(\mathbf{x}))^2} \right) & \text{if } r(\mathbf{x}) < 1 , \\ 0 & \text{otherwise} \end{cases} \quad (4.40)$$

with $r(\mathbf{x}) = \frac{\|\mathbf{x}_0 - \mathbf{x}\|}{0.74}$ and $\mathbf{x}_0 = (1, 0, 0)^T$. Table 1 shows that the second-order accuracy of the numerical solution is achieved.

4.2 Diffusion on a sphere

We next simulate the diffusion of a material on a sphere of radius r and centered at the origin of the spherical coordinate specified by ϕ , θ and $r = 1$ [32]. The initial condition and the exact solution to the diffusion equation on the surface

$$\frac{\partial f}{\partial t} = \Delta_{\Gamma} f, \quad t \in (0, 0.02] \quad (4.41)$$

is given by

$$f(\phi, \theta, t) = (\sin^5(\theta) \cos(5\phi) + \sin^4(\theta) \cos(\theta) \cos(4\phi)) \exp(-30t/r^2). \quad (4.42)$$

Table 2 shows the numerical errors and the second-order of accuracy of the solution.

4.3 Convection-diffusion on a sphere

Motivated by test problems in [16], we consider to solve on the unit sphere \mathbb{S}_1 convection-diffusion problem described by

$$\frac{\partial u}{\partial t} + \nabla_{\Gamma} \cdot (u\mathbf{V}) = a\Delta_{\Gamma} u + s. \quad (4.43)$$

The divergence-free advecting velocity field $\mathbf{V} = (v_1, v_2, v_3)^T$ at position $\mathbf{x} = (x_1, x_2, x_3)^T$ is given by $\mathbf{V} = \frac{2\pi}{\|\mathbf{x}\|} (x_2, -x_1, 0)^T$. In the spherical coordinate system (θ, ϕ) , defined by

$$\mathbf{x} = (r \sin \theta \cos \phi, r \sin \theta \sin \phi, r \cos \theta)^T$$

for $\theta \in [0, \pi]$ and $\phi \in [0, 2\pi)$, the exact solution to this problem is chosen to be

$$u(\mathbf{x}, t) = \exp(-t) \sin^2(\theta) \cos^2(\phi).$$

Value of the diffusion coefficient a is set to be 0.05. The source term function s is chosen such that $u(\mathbf{x}, t)$ satisfies Eq. (4.43) exactly. Table 3 shows the numerical errors and the second-order accuracy of the numerical solution to problem (4.43).

4.4 Cahn-Hilliard equation on surfaces

In this set of numerical simulations, we set $\Psi'(u) = u^3 - u$, $b(u) = 1.0$, and $\gamma = 0.008$ as in [15]. The tests are done on different surfaces. The initial condition for all simulations is randomly generated. The first simulation is performed on the unit spherical surface \mathbb{S}_1 ; the second simulation is done on an ellipsoid defined by

$$\mathbb{S}_2 = \left\{ \mathbf{x} \in \mathbb{R}^3 \mid \frac{x_1^2}{4} + \frac{x_2^2}{1} + \frac{x_3^2}{1.5^2} = 1 \right\};$$

Table 1 Numerical errors and convergence order for u_h of the DG method for solving the problem (4.39).

h	L_1	order	L_{∞}	order
0.2	1.21E-3	-	3.77E-3	-
0.1	3.04E-4	1.99	7.70E-4	2.29
0.05	5.63E-5	2.43	1.74E-4	2.15
0.025	1.00E-5	2.49	3.43E-5	2.34

Table 2 Numerical errors and convergence order of the LDG method for solving Eq. (4.41).

h	L_1	order	L_{∞}	order	L_2	order
0.1	2.93E-2	-	2.02E-2	-	1.23E-2	-
0.05	7.13E-3	2.04	5.73E-3	1.82	3.02E-3	2.03
0.025	1.75E-3	2.03	1.36E-3	2.07	7.43E-4	2.02
0.0125	4.38E-4	2.00	3.74E-4	1.86	1.85E-4	2.01

Table 3 Numerical errors and convergence order of the LDG method for solving Eq. (4.43).

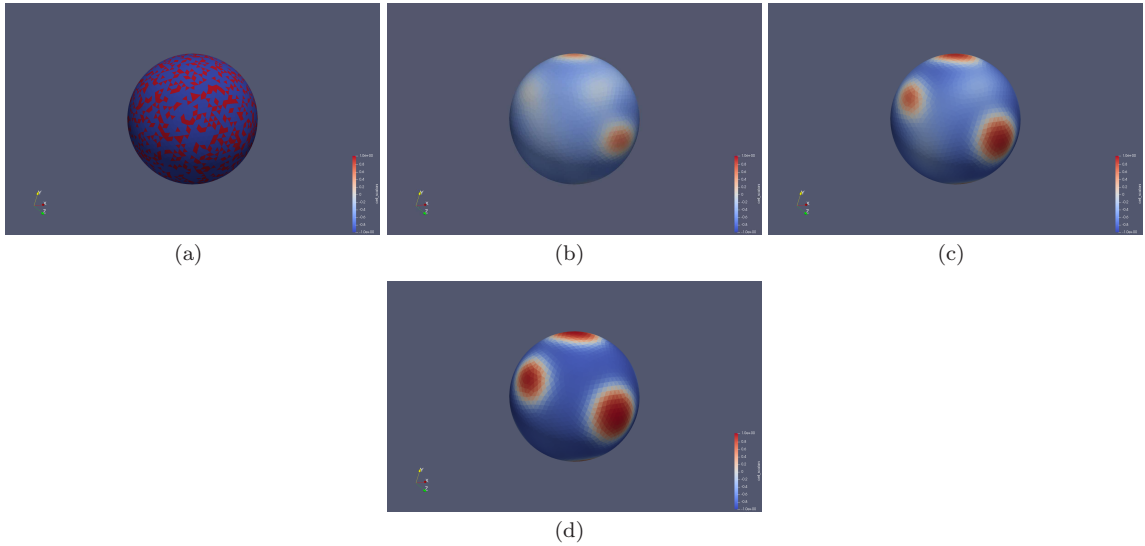
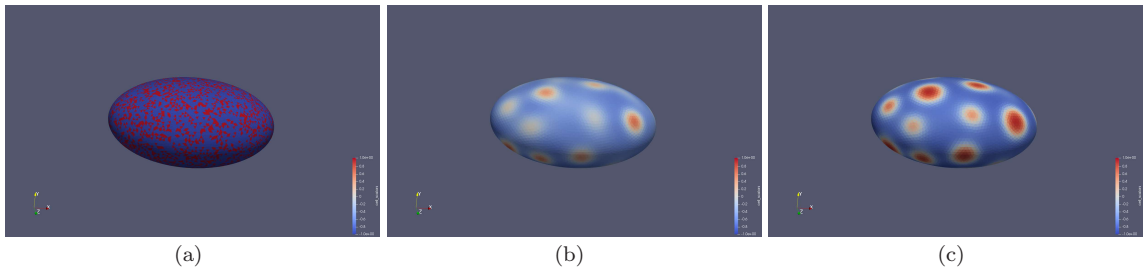
h	L_1	order	L_∞	order
0.1	5.67E-3	-	1.35E-3	-
0.05	1.36E-3	2.06	3.48E-4	1.96
0.025	3.35E-4	2.02	8.98E-5	1.95
0.0125	8.33E-5	2.01	2.28E-5	1.98

and the third simulation is performed on a biconcave surface defined by

$$\mathbb{S}_3 = \left\{ \mathbf{x} \in \mathbb{R}^3 \mid x_3^2 - 0.25R_0^2 \left(1 - \frac{x_1^2 + x_2^2}{R_0^2} \right) \left(C_0 + C_1 \frac{x_1^2 + x_2^2}{R_0^2} + C_2 \frac{x_1^2 + x_2^2}{R_0^2} \right)^2 = 0 \right\},$$

where $R_0 = 1.4$, $C_0 = 0.207161$, $C_1 = 2.002558$ and $C_2 = -1.122762$.

Figures 2, 3 and 4 show simulation results. We can observe that initially randomly generated patterns gradually merge into large structures as expected.

**Fig. 2** Numerical solutions of the concentration u at time $t = 0.0, 0.1, 0.2, 0.3$ on unit sphere \mathbb{S}_1 with 2964 nodes and 5924 triangles.**Fig. 3** Numerical solutions of the concentration u at time $t = 0.0, 0.1, 0.2$ on ellipsoid \mathbb{S}_2 triangulated with 6374 nodes and 12744 triangles.

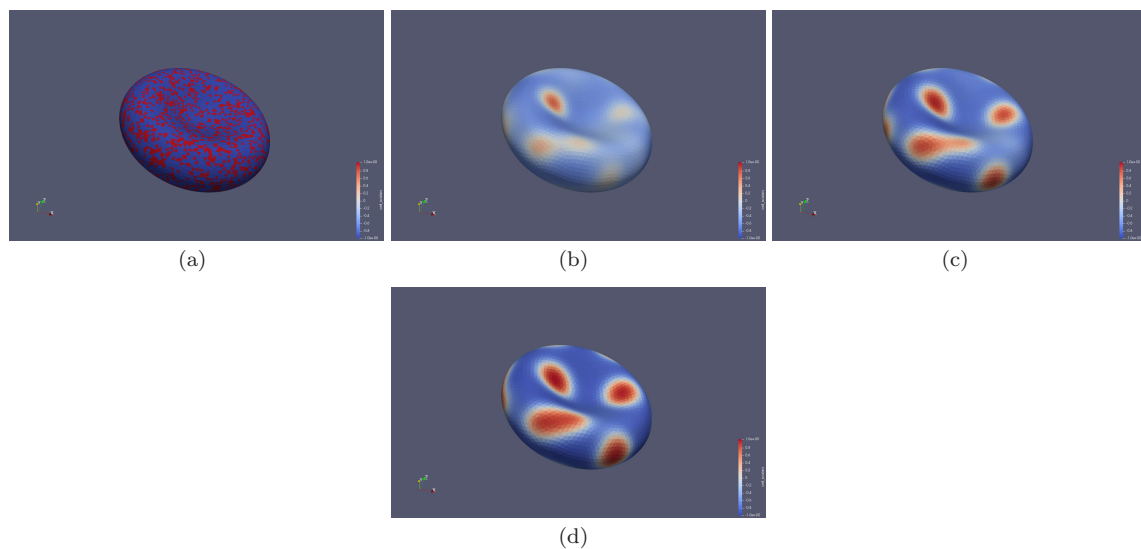


Fig. 4 Numerical solutions of the concentration u at time $t = 0.0, 0.1, 0.2, 0.3$ on biconcave surface \mathbb{S}_3 with 3904 nodes and 7804 triangles.

5 Conclusion

In this paper we introduced LDG schemes for solving initial value problems posed on closed smooth surfaces, which are triangulated by planar triangles. Because of the planar triangle approximation of smooth surfaces, the schemes are second-order accurate. To further improve order of accuracy of the LDG schemes on surfaces, curved triangles are needed for discretization. While this paper only implements the second-order accurate schemes, the proposed schemes in principle can be generalized to meshes consisting of curved elements. However, this would significantly increase programming complexity. We will report in a subsequent paper implementation of these schemes with higher-order accuracy.

Lastly, we used a $C_{CFL} \leq 0.1$ in our simulations, which is much smaller than that of LDG for planar domain problems. We will investigate how curvature of the surface affects the CFL condition in the future.

6 Acknowledgement

References

1. D. ADALSTEINSSON, J.A. SETHIAN, Transport and diffusion of material quantities on propagating interfaces via level set methods, *J. Comput. Phys.*, 185(1), 271–288 (2003).
2. V. AIZINGER, L. BUNBERT, AND M. FRIED., Comparison of two local discontinuous Galerkin formulations for the subjective surfaces problem *Computing and Visualization in Science*, 18(6):193-202 (2018)
3. M. BERGDORF, I. SBALZARINI, P. KOUMOUTSAKOS, A Lagrangian particle method for reaction-diffusion systems on deforming surfaces, *J. Math. Biol.*, 61, 649–663 (2010).
4. A. BERTOZZI, S. ESEDOGLU, AND A. GILLETTE, Inpainting of binary images using the Cahn-Hilliard equation, *IEEE Trans. Image Process.*, 16:285–291, 2007.
5. M. BERTALMIO, L. CHENG, S. OSHER AND G. SAPIRO, Variational problems and partial differential equations on implicit surfaces, *J. Comput. Phys.*, 174, 759–780,2001.
6. S.BOSCARINO, F. FILBET, AND G. RUSSO, High order semi-implicit schemes for time dependent partial differential equations, *J. Sci. Comput.* 68(3): 975-1001, (2016).
7. B. COCKBURN AND A. DEMLOW, Hybridizable Discontinuous Galerkin and Mixed Finite Element Methods for Elliptic Problems on Surfaces, *Math. Comput.*, 85(302):2609–2638, (2016).
8. B. COCKBURN, G. KANSCHAT, I. PERUGIA AND D. SCHÖTZAU, Superconvergence of the Local Discontinuous Galerkin Method for Elliptic Problems on Cartesian Grids, *SIAM J. Numer. Anal.*, 39(1):264–285, (2001).
9. B. COCKBURN AND C.-W. SHU, The Local Discontinuous Galerkin Method for Time-Dependent Convection-Diffusion Systems, *SIAM J. Numer. Anal.*, 35(6):2440–2463, (1998).
10. D.N. ARNOLD, F. BREZZI, B. COCKBURN AND L.D. MARINI, Unified Analysis of Discontinuous Galerkin Method for Elliptic Problems, *SIAM J. Numer. Anal.*, 39(5):1749–1779, (2002).

11. A. DEDNER, P. MADHAVAN, AND B. STINNER, Analysis of the Discontinuous Galerkin Method for Elliptic Problems on Surfaces, *IMA J. Numer. Anal.*, 53(2):1145–1171, (2013).
12. A. DEDNER AND P. MADHAVAN, Discontinuous Galerkin methods for hyperbolic and advection-dominated problems on surfaces, [arXiv:1505.06752](https://arxiv.org/abs/1505.06752), (2015).
13. Q. DU, C. LIU, AND X. WANG, A phase field approach in the numerical study of the elastic bending energy for vesicle membranes, *J. Comput. Phys.*, 198:450–468, (2004).
14. Q. DU, L. JU, AND T. LI, Analysis of a mixed finite-volume discretization of fourth-order equations on general surfaces, *IMA J. Numer. Anal.*, 29:376–403, (2009).
15. Q. DU, L. JU, AND T. LI, Finite Element Approximation of the Cahn-Hilliard Equation on Surfaces, *Computer Methods in Applied Mechanics and Engineering*, 200(29-32):2458–2470, (2011).
16. Q. DU AND L. JU, Finite Volume Methods on Spheres and Spherical Centroidal Voronoi Meshes, *SIAM J. Numer. Anal.*, 43(4):1673–1692, (2005).
17. Q. DU AND L. JU, Approximations of a Ginzburg-Landau Model for Superconducting Hollow Spheres Based on Spherical Centroidal Voronoi Tessellations, *Math. Comput.*, 74:1257–1280, (2005).
18. G. DZIUK Finite elements for the Beltrami operator on arbitrary surfaces, *Partial differential equations and calculus of variations*, 142-155, (1988).
19. G. DZIUK AND C. M. ELLIOTT, Surface Finite Elements for Parabolic Equations, *J. Comput. Math.*, 25:385–407, (2007).
20. G. DZIUK, Computational Parametric Willmore Flow, *Numer. Math.*, 111:55–80, (2008).
21. G. DZIUK AND C. M. ELLIOTT, Finite Element Methods for Surface PDEs, *Acta Numerica*, 289–396, (2013).
22. P.F. ANTONIETTI, A. DEDNER, P. MADHAVAN, S. STANGALINO, B. STINNER AND M. VERANI, High Order Discontinuous Galerkin Methods for Elliptic Problems on Surfaces, *SIAM J. Numer. Anal.*, 53(2):1145–1171, (2015).
23. E. J. FUSELIER, G. B. WRIGHT, A High-Order Kernel Method for Diffusion and Reaction-Diffusion Equations on Surfaces, *J. Sci. Comput.*, 56:535–565, (2013)
24. R. GUO, F. FILBET AND Y. XU, Efficient high order semi-implicit time discretization and local discontinuous Galerkin methods for highly nonlinear PDEs, *J. Sci. Comput.* 68(3):1029-1054, (2016).
25. F.X. GIRALDO, Lagrange-Galerkin Methods on Spherical Geodesic Grids, *J. Comput. Phys.*, 136(2):197–213, (1997).
26. J. GIESSELMANN, A convergence result for finite volume schemes on Riemannian manifolds, *Math. Model. Numer. Anal.*, 43(5):929–955 (2009).
27. J. GIESSELMANN AND T. MÜLLER, Geometric error of finite volume schemes for conservation laws on evolving surfaces, *Numer. Math.*, 128:489–516, (2014).
28. S. GOTTLIEB AND C.-W. SHU, Total Variation Diminishing Runge-Kutta Schemes, *Mathematics of Computation*, 67(221):73-85, (1998).
29. J.B GREER, An improvement of a recent Eulerian method for solving PDEs on general geometries, *J. Sci. Comput.*, 29, 321–352 (2006).
30. P.G. LEFLOCH, B. OKUTMUSTUR, W. NEVES, Hyperbolic conservation laws on manifolds. An error estimate for finite volume schemes, *Acta Math. Sin. (Engl. Ser.)*, 25(7):1041–1066 (2009).
31. M. LENZ, S.F. NEMADJIEU, M. RUMPF, A convergent finite volume scheme for diffusion on evolving surfaces, *SIAM J. Numer. Anal.*, 49(1):15–37 (2011).
32. S. LEUNG, J. LOWENGRUB AND H. ZHAO, A grid based particle method for solving partial differential equations on evolving surfaces and modeling high order geometrical motion, *J. Comput. phys.*, 230:2540–2561, (2011).
33. X. LI, J. LOWENGRUB, A. RATZ, A. VOIGT Solving PDEs in complex geometries: a diffuse domain approach *Comm. Math. Sci.*, 7 (1), 81, (2009)
34. C.B.MACDONALD, S.J. RUUTH, Level set equations on surfaces via the closest point method, *J. Sci. Comput.*, 35, 219–240 (2008)
35. C.B.MACDONALD, S.J. RUUTH, The implicit closest point method for the numerical solution of partial differential equations on surfaces, *SIAM J. Sci. Comput.*, 31, 4330–4350 (2009)
36. M. MEHRA, AND K.-R. KEVLAHAN, An adaptive Wavelet Collocation Method for the Solution of Partial Differential Equations on the Sphere, *J. Comput. phys.*, 227(11):5610–5632, (2008).
37. I. NITSCHKE, A. VOIGT, AND J. WENSCH, A finite element approach to incompressible two-phase flow on manifolds, *J. Fluid Mech.* 708: 418-438, (2012).
38. I. L. NOVAK, F. GAO, Y. S. CHOI, D. RESASCO, J. C. SCHAFF, AND B. M. SLEPCHENKO, Diffusion on a curved surface coupled to diffusion in the volume: Application to cell biology, *J. Comput. phys.*, 226(2), 1271-1290, (2007).
39. P.-O. PERSSON AND G. STRANG, A Simple Mesh Generator in MATLAB, *SIAM Review*, 46(2), 329-345, (2004).
40. J. PERAIRE AND P.-O. PERSSON, The Compact Discontinuous Galerkin (CDG) Method for Elliptic Problems, *SIAM J. Sci. Comput.*, 30(4), 1806-1824, (2008).
41. C. PIRET, The orthogonal gradients method: a radial basis functions method for solving partial differential equations on arbitrary surfaces, *J. Comput. Phys.*, 231(20), 4662–4675 (2012)
42. A. RATZ, A. VOIGT PDE's on surfaces—a diffuse interface approach *Comm. Math. Sci.*, 4(3), 575-590 (2006).
43. R. V. ROY, A. J. ROBERTS, AND M. E. SIMPSON, A lubrication model of coating flows over a curved substrate in space, *J. Fluid Mech.* 454: 235-261, (2002)
44. S.J. RUUTH, B. MERRIMAN, A simple embedding method for solving partial differential equations on surfaces, *J. Comput. Phys.* 227, 1943–1961 (2008)
45. I.F. SBALZARINI, A. HAYER, A. HELENIUS, P. KOUMOUTSAKOS, Simulations of (an)isotropic diffusion on curved biological surfaces. *Biophys. J.* 90, 878–885 (2006)
46. P. SCHWARTZ, D. ADALSTEINSSON, P. COLELLA, A.P. ARKIN, M. ONSUM, Numerical computation of diffusion on a surface, *Nat. Acad. Sci.*, 102(32), 11151–11156 (2005)
47. V. SHANKAR, G. B. WRIGHT, R. M. KIRBY AND A. L. FOGELSON, A Radial Basis Function (RBF)-Finite Difference (FD) Method for Diffusion and Reaction-Diffusion Equations on Surfaces, *J. Sci. Comput.*, 63:745–768, (2015).

48. C.-W. SHU AND S. OSHER, Efficient implementation of essentially non-oscillatory capturing schemes, J. Comput. Phys., 77:439-471, (1988).
49. P. SUCHDEA, J. KUHNERT A Fully Lagrangian Meshfree Framework for PDEs on Evolving Surfaces arXiv:1902.08107v2, (2019)
50. J.A. PUDYKIEWICZ, Numerical Solution of the Reaction-Advection-Diffusion Equation on the Sphere, J. Comput. phys., 213:358-390, (2006).
51. P. SCHWARTZ, D. ADALSTEINSSON, P. COLELLA, A.P. ARKIN AND M. ONSUM, Numerical computation of diffusion on a surfaces, PNAS., 102(32):1151-11156, (2005).
52. Y. XU AND C.-W. SHU, Local Discontinuous Galerkin Method for Surface Diffusion and Willmore Flow of Graphs, J. Sci. Comput., 40: 375-390, (2009).
53. J. YAN AND C.-W. SHU, Local Discontinuous Galerkin Methods for Partial Differential Equations with Higher Order Derivatives, J. Sci. Comput., 17(1-4):27-47, (2002).
54. C.-W. SHU AND S. OSHER, Efficient implementation of essentially non-oscillatory capturing schemes, J. Comput. Phys., 77:439-471, (1988).
55. X. XIA, Y. XU AND C.-W. SHU, Local Discontinuous Galerkin Methods for the Cahn-Hilliard Type Equations, J. Comput. Phys., 227:472-491, (2007).
56. D.L. WILLIAMSON, J.B. DRAKE, J.J. HACK, R. JAKOB, P.N. SWARZTRAUBER, A standard test set for numerical approximations to the shallow water equations in spherical geometry, J. Comput. Phys., 102(1):211-224 (1992).
57. F. ZHANG, Y. XU, F. CHEN, R. GUO, Interior Penalty Discontinuous Galerkin Based Isogeometric Analysis for Allen-Cahn Equations on Surfaces, Commun. Comput. Phys., 18: 1380-1416 (2015).
58. F. ZHANG, Y. XU, F. CHEN, , Discontinuous Galerkin Based Isogeometric Analysis for Geometric flows, J. Sci. Comput., 71: 525-546 (2017).
59. T. CHEN, C.-W. SHU, , Review of entropy stable discontinuous Galerkin methods for systems of conservation laws on unstructured simplex meshes, Conference Proceedings, (2019).
60. H. WANG, C.-W. SHU, Q. ZHANG, Stability analysis and error estimates of local discontinuous Galerkin methods with implicit-explicit time-marching for nonlinear convection-diffusion problems, Appl. Math. Comput., 272: 237-258, (2016).

A Nonlinear Surface Transport

We consider nonlinear transport equation on a closed manifold

$$\frac{\partial u}{\partial t} + \nabla_{\Gamma} \cdot (\mathbf{f}(u)) = 0. \quad (1.44)$$

The flux \mathbf{f} is some smooth vector field tangent to Γ . We want to show that the DG scheme is stable for solving Eq. (1.44) on manifold. The proof follows [59,60]. The main difficulty of the proof is due to the fact that co-normals of two neighboring elements are not the same, i.e. $\mathbf{n}^I \neq -\mathbf{n}^E$, \mathbf{n}^I and \mathbf{n}^E are co-normals defined on the edge shared by the neighboring elements. See also Fig. 1

The DG method for solving Eqs. (1.44) is defined by: Find $u_h \in \mathbb{S}_{h,k}$, such that for all test functions $v_h \in \mathbb{S}_{h,k}$,

$$\int_{\mathbf{K}_h} (u_h)_t v_h \, d\mathbf{x} - \int_{\mathbf{K}_h} \mathbf{f}(u) \cdot \nabla_{\Gamma_h} v_h \, d\mathbf{x} + \int_{\mathbf{K}_h} (\beta_h u_h v_h) \, d\mathbf{x} + \int_{\partial \mathbf{K}_h} \widehat{f}_h v_h \, ds = 0, \quad (1.45)$$

where \widehat{f}_h is the numerical flux and defined as

$$\widehat{f}_h = \widehat{f_{K_h}}(u_h^E, u_h^I, \mathbf{n}^E, \mathbf{n}^I) = \{\mathbf{f}(u_h), \mathbf{n}_h\} + \frac{\alpha}{2} \llbracket u_h \rrbracket = \frac{1}{2} (\mathbf{f}(u_h^I) \cdot \mathbf{n}^I - \mathbf{f}(u_h^E) \cdot \mathbf{n}^E) - \frac{\alpha}{2} (u_h^E - u_h^I), \quad (1.46)$$

with $\alpha = \max_i |\sum_i f'_i n_i|$.

Lemma 2 If the numerical flux is defined as (1.46), it is

- consistent, $\widehat{f_{K_h}}(u_h, u_h, \mathbf{n}, \mathbf{n}) = \mathbf{f}(u_h) \cdot \mathbf{n}$;
- conservative, $\widehat{f_{K_h}}(u_h^E, u_h^I, \mathbf{n}^E, \mathbf{n}^I) = -\widehat{f_{K_h}}(u_h^I, u_h^E, \mathbf{n}^I, \mathbf{n}^E)$;
- monotone, non-decrease with u_h^I and non-increase with u_h^E under a suitable α .

If there exists an entropy flux $F_i(u)$ such that

$$U'(u) f'_i(u) = F'_i, \quad i = 1, 2, 3, \quad (1.47)$$

then the convex function $U(u)$ is called an entropy function for Eq. (1.44). If we denote $v(u) = U'(u)$ and

$$\psi_i(v) = v f_i(u(v)) - F_i(u(v)), \quad (1.48)$$

it is easy to check that

$$\psi'_i(v) = f_i(u(v)). \quad (1.49)$$

Definition 4 A numerical flux $\widehat{f}(u_h^E, u_h^I, \mathbf{n}^E, \mathbf{n}^I)$ is called entropy stable with respect to some entropy U if it is consistent, single-valued and satisfies the following inequality

$$(v^E - v^I)\widehat{f}(u_h^E, u_h^I, \mathbf{n}^E, \mathbf{n}^I) \leq \sum_i (\psi_i(u_h^E)n_i^E + \psi_i(u_h^I)n_i^I) \quad (1.50)$$

Theorem 3 If $U = \frac{u^2}{2}$ is an entropy function of (1.44), and \widehat{f} is entropy stable with respect to U , then DG method (1.45) is L^2 stable in the sense that

$$\frac{d}{dt} \left(\sum_{K_h} \int_{\mathbf{K}_h} \frac{(u_h^I)^2}{2} dx \right) \leq 0 \quad (1.51)$$

Proof: Taking $v_h = u_h$ and summing over all elements yields

$$\begin{aligned} & \frac{d}{dt} \left(\sum_{K_h} \int_{\mathbf{K}_h} \frac{(u_h^I)^2}{2} dx \right) \\ &= \sum_{K_h} \int_{\mathbf{K}_h} \mathbf{f}(u) \cdot \nabla_{\Gamma_h} u_h dx - \sum_{K_h} \int_{\partial K_h} \widehat{f}_h u_h^I ds \\ &= \sum_{K_h} \int_{\partial K_h} (\psi_i(u_h^I)n_i^I - \widehat{f}_h u_h^I) ds \\ &= \sum_{e \in \mathcal{E}} \int_e (\psi_i(u_h^I)n_i^I + \psi_i(u_h^E)n_i^E + \widehat{f}_h(u_h^E - u_h^I)) ds \leq 0. \end{aligned} \quad (1.52)$$

Question: how to design an entropy stable numerical flux? If we use the Lax-Friedrich flux (1.46), I could not prove it is an entropy stable flux with respect to entropy $U = \frac{u^2}{2}$ since the conormals of two neighbor elements are not same.

When $U = \frac{u^2}{2}$, we have $v = u$, and $\psi_i = u f_i - F_i$.

$$\begin{aligned} & (v_h^E - v_h^I)\widehat{f}_{K_h}(u_h^E, u_h^I, \mathbf{n}^E, \mathbf{n}^I) \\ &= (u_h^E - u_h^I)\widehat{f}_{K_h}(u_h^E, u_h^I, \mathbf{n}^E, \mathbf{n}^I) \\ &= \frac{1}{2}(u_h^E - u_h^I)(\mathbf{f}(u_h^I) \cdot \mathbf{n}^I - \mathbf{f}(u_h^E) \cdot \mathbf{n}^E) - \frac{\alpha}{2}(u_h^E - u_h^I)^2 \end{aligned} \quad (1.53)$$

$$\begin{aligned} &= \frac{1}{2}(\mathbf{f}(u_h^I) \cdot \mathbf{n}^I u_h^E - \mathbf{f}(u_h^I) \cdot \mathbf{n}^I u_h^I - \mathbf{f}(u_h^E) \cdot \mathbf{n}^E u_h^E + \mathbf{f}(u_h^E) \cdot \mathbf{n}^E u_h^I) - \frac{\alpha}{2}(u_h^E - u_h^I)^2 \\ &= ?? \end{aligned} \quad (1.54)$$

